

VLM-CAD: VLM-Optimized Collaborative Agent Design Workflow for Analog Circuit Sizing

1st Guanyuan Pan

Hangzhou Dianzi University
Hangzhou, China
guanyuanpeterpan@gmail.com

2nd Yugui Lin

SCBC, Guangdong University of Foreign Studies
Guangzhou, China
yuguilin0209@163.com

3rd Tiansheng Zhou

Hangzhou Dianzi University
Hangzhou, China
zhoutiansheng_2024@163.com

4th Pietro Liò

University of Cambridge
Cambridge, United Kingdom
pl219@cam.ac.uk

5th Shuai Wang

Hangzhou Dianzi University
Hangzhou, China
shuaiwang.tai@gmail.com

6th Yaqi Wang*

Hangzhou Dianzi University
Hangzhou, China
wangyaqi@hdu.edu.cn

Abstract—Analog mixed-signal circuit sizing involves complex trade-offs within high-dimensional design spaces. Existing automatic analog circuit sizing approaches often underutilize circuit schematics and lack the explainability required for industry adoption. To tackle these challenges, we propose a Vision Language Model-optimized collaborative agent design workflow (VLM-CAD), which analyzes circuits, optimizes DC operating points, performs inference-based sizing and executes external sizing optimization. We integrate Image2Net to annotate circuit schematics and generate a structured JSON description for precise interpretation by Vision Language Models. Furthermore, we propose an Explainable Trust Region Bayesian Optimization method (ExTuRBO) that employs collaborative warm-starting from agent-generated seeds and offers dual-granularity sensitivity analysis for external sizing optimization, supporting a comprehensive final design report. Experiment results on amplifier sizing tasks using 180nm, 90nm, and 45nm Predictive Technology Models demonstrate that VLM-CAD effectively balances power and performance, achieving a 100% success rate in optimizing an amplifier with a complementary input and a class-AB output stage, while maintaining total runtime under 43 minutes across all experiments.

Index Terms—Analog Circuit Sizing, Agentic AI, Vision Language Model, Explainability, Electronic Design Automation

I. INTRODUCTION

Analog and mixed-signal (AMS) integrated circuits are essential components in electronic systems [11]. However, designing AMS circuits is complex and time-consuming. AMS circuit designers must often trade off Power, Performance, and Area to achieve balanced circuit performance, relying solely on experience. In the design process for AMS circuits, circuit sizing is particularly challenging. It involves an iterative process that balances competing objectives across various requirements, all within a high-dimensional design space. As a result, automatic circuit sizing has attracted significant research interest due to its ability to rapidly explore a wide range of design variables to identify optimal size combinations.

The evolution of automatic analog circuit sizing approaches has seen significant advancements over the years. Early efforts

included Expert Systems (ES) and Machine Learning (ML) methods [18], [19] such as Genetic Algorithms (GA) [12] and Bayesian Optimization (BO) [13], [17]. Reinforcement Learning (RL) has also shown promise [14].

Language models, including Large Language Models (LLMs) and Vision Language Models (VLMs), have recently demonstrated exceptional capabilities across a range of tasks, such as code generation and multimodal reasoning. These models could propose circuit optimization strategies and analyze simulation data [2], [3]. To integrate language models with external tools, agentic workflows are becoming increasingly prominent, with engineers applying them to various tasks including automatic analog circuit sizing [4], [5].

However, current automatic analog circuit sizing approaches have the following challenges:

- **Circuit schematic underutilization:** Analog circuit schematics are vital for analog circuit designers to understand the structures and functions of transistor-level circuit netlists [15]. However, to our knowledge, no automatic analog circuit sizing approaches leverage schematics for circuit analysis or parameter optimization.
- **Nonexistent or hallucinated explainability:** ES, ML, and RL methods are black-box methods that deliver solutions with no insights into their internal workings. While using language models for automatic analog circuit sizing offers some level of explainability [5], this is questionable due to their tendency to hallucinate [16].

To overcome these challenges,

- 1) We propose **VLM-CAD**, a VLM-optimized collaborative agent design workflow for analog circuit sizing.
- 2) We introduce circuit schematics as inputs for automatic circuit sizing. Specifically, we use Image2Net to annotate schematics and extract component information and connections, which assist VLM in interpreting them.
- 3) We propose **ExTuRBO**, an Explainable Trust Region Bayesian Optimization method that collaboratively warm-starts local search to accelerate convergence

*Corresponding Author.

and utilizes Automatic Relevance Determination (ARD) lengthscales to support a dual-granularity sensitivity report.

We demonstrated VLM-CAD in Fig. 1. We apply VLM-CAD to two distinct circuits using Predictive Technology Model (PTM) nodes to optimize six performance metrics [10]. The first circuit is an amplifier with a complementary input and a class-AB output stage, which we test for both 180nm and 90nm processes. The second circuit is a two-stage Miller operational amplifier at 45nm. For each circuit, VLM-CAD achieves excellent or satisfactory results.

II. RELATED WORK

A. Machine Learning and Reinforcement Learning Methods

ML techniques have shown their potential in automatic analog circuit sizing [18], [19]. BO treats transistor sizing as an optimization problem, with the objective function evaluated via simulation. It utilizes Gaussian Process (GP) regression to guide the search for high-performing solutions efficiently [13]. RL further enhances sizing efficiency by leveraging rewards from iterative simulations, enabling better adaptation to complex design spaces [14]. However, these methods have high computational costs and inconsistent performance across different circuit designs and performance metrics [17], [18]. Additionally, their lack of explainability poses a significant barrier to their adoption in the industry, as designers are often suspicious of solutions they cannot interpret [19].

B. LLM-based Methods and Agentic Workflows

Recently, LLMs have demonstrated their capabilities to optimize analog circuits. LEDRO [2] utilized LLMs alongside optimization techniques to iteratively refine the design space for analog circuit sizing. LLMACD [3] utilized a refined prompt manager to extract circuit representation, embed circuit knowledge, and model the knowledge-intensive design process within a Chain-of-Thought workflow. Nevertheless, LLMs have a limited understanding of AMS circuit topologies [20], making it challenging to capture the trade-offs that affect circuit performance. Additionally, their lack of mathematical precision undermines the reliability of sizing and performance estimation, underscoring the need for seamless integration with external tools, such as simulators [21].

To address these challenges in analog design, agentic workflows are becoming more prominent. AmpAgent [4] efficiently designs multi-stage amplifiers from essays using three LLM-based agents to handle process and specifications. AnaFlow [5] replicates the workflow of expert designers by introducing a multi-agent LLM workflow that provides structured reasoning and explainability in the process.

C. Circuit Schematics and VLM

Circuit schematics are a core element of analog circuit design, as they contain information about circuit components and their connections. Schematics visually depict the structure and interconnections of a circuit, providing designers with an intuitive reference for understanding how it operates [15].

However, existing schematic resources are underutilized and have not been accurately transformed into suitable structured information for circuit simulation.

VLMs have the potential to understand circuit diagrams, offering unique advantages for handling legacy design documents and generating layouts, thereby garnering attention in the field. CURVLM [6] applies Group Relative Policy Optimization to fine-tune the VLM to interpret digital circuit diagrams. [7] introduce CoRe-VLM, a refinement framework inspired by actor-critic methods for schematic Visual Question Answering, along with SchemixQA, a multimodal benchmark designed to evaluate VLMs on technical schematics. However, existing methods still struggle to interpret circuit diagrams, demonstrating insufficient accuracy and thus are not reliable for automatic circuit sizing [1], [22].

III. VLM-CAD AGENTIC WORKFLOW

A. Image2Net Interpreting Circuit Schematic

Despite excellent performance on object detection and complex multimodal reasoning tasks, VLMs struggle to count intersections in line diagrams or identify geometric relationships among intersecting circles [1]. This limitation raises concerns about their ability to interpret schematic diagrams and understand circuit connectivity.

We therefore utilize Image2Net¹, a hybrid framework combining DL-based object detection with heuristic computer vision algorithms to annotate the schematic and extract information about components and their connections.

- **Component Detection:** We employ a fine-tuned YOLOv8-Pose model to identify the bounding boxes of components and predict the coordinates of terminal poses. We then align these coordinates with the nearest wire pixels to ensure accurate anchoring.
- **Corner Detection:** To effectively capture the wiring topology, we apply a combination of feature detection algorithms, including Harris, Shi-Tomasi, Oriented FAST and Rotated BRIEF, Scale-Invariant Feature Transform, and Binary Robust Invariant Scalable Keypoints, to maximize corner detection recall. We then employ Density-Based Spatial Clustering of Applications with Noise clustering to merge any duplicate detections.
- **Graph Construction:** Next, we create a connectivity graph by verifying pixel-level continuity between component pins and corners in the binarized schematic. We verify this using a hybrid approach: we employ efficient vectorized array slicing to validate orthogonal connections, and Bresenham's algorithm to trace diagonal paths. We then aggregate the validated segments to form graph edges, clustering all physically connected nodes into distinct electrical nets.
- **Annotated Schematic and JSON Description Generation:** Finally, we parse the resulting graph to map

¹Image2Net was proposed by Yiren Pan (panyiren@hdu.edu.cn) and won the first prize of the 2024 China Postgraduate IC Innovation Competition - EDA Elite Challenge Contest.

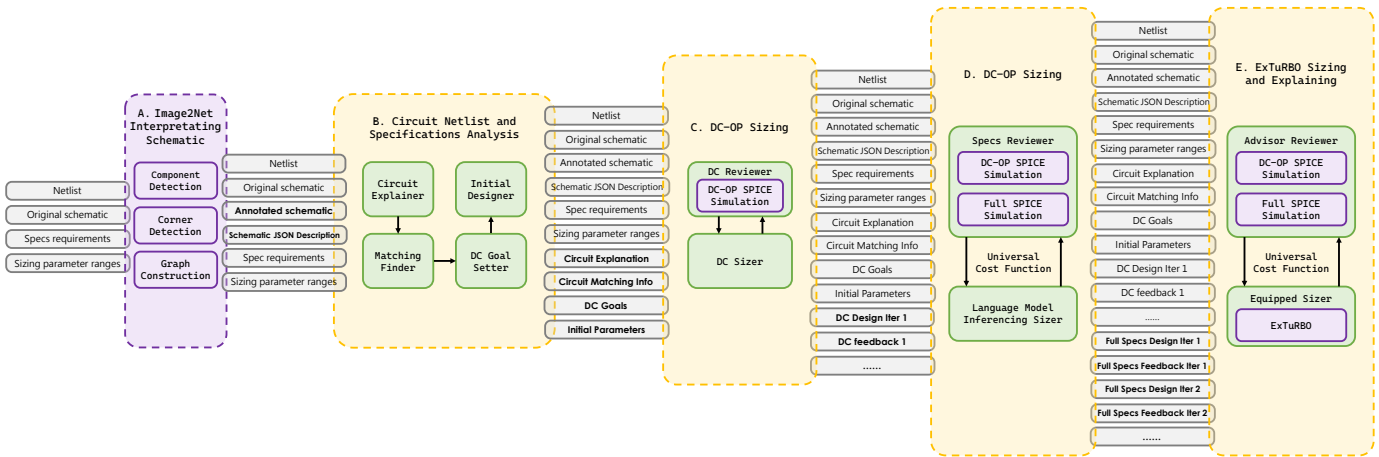


Fig. 1: VLM-CAD overview. We include five stages for VLM-CAD: A. Image2Net Interpreting Circuit Schematic (see Sec. III-A), B. Circuit Netlist and Specifications Analysis (see Sec. III-B), C. DC-OP Sizing (see Sec. III-C), D. Inference-Only Sizing (see Sec. III-D) and E. Sizing and Explaining (see Sec. III-E).

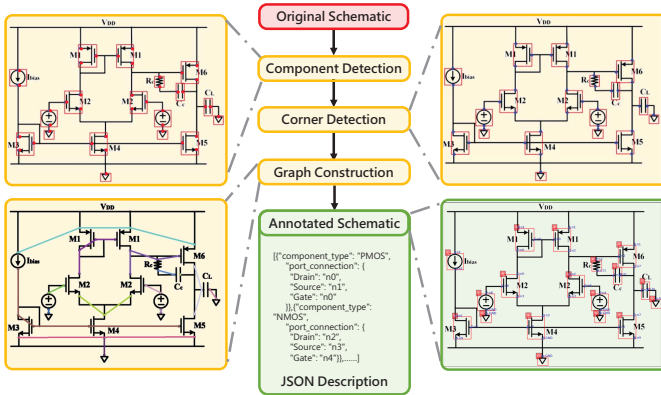


Fig. 2: Image2Net for circuit schematic interpretation, including three stages: Component Detection, Corner Detection, and Graph Construction (see Sec. III-A).

component ports to net identifiers, generating a JSON description of the schematic that includes its components and their connections. Additionally, we create an annotated schematic that color-codes the distinct electrical connections for verification.

We demonstrate this phase in Fig. 1.A and present further details in Fig. 2.

B. Circuit Netlist and Specifications Analysis

After annotating the schematic and extracting information about components and their connections, we conduct a deep analysis of the analog circuit sizing problem using a sequence of specialist agents, thereby decomposing the complex task.

- **Circuit Explainer:** This VLM Agent serves as the cognitive foundation of the workflow. It ingests both the circuit schematic images and the SPICE netlist, along with performance specifications. Beyond basic connectivity analysis, it leverages visual and textual data to identify

analog sub-blocks, such as differential pairs and current mirrors, deduce signal flow and feedback mechanisms, and synthesize a holistic understanding of the circuit's operation. This high-level analysis provides the necessary context for all subsequent sizing and optimization agents.

- **Matching Finder:** Leveraging both the schematic and the netlist, this VLM agent identifies transistor clusters that require precise symmetry. Notably, it goes beyond simple grouping by explicitly defining parameter-level constraints for each group. It also infers layout implications, for instance, needs for interdigitation, and provides the engineering rationale for these constraints, ensuring the subsequent sizing process respects the physical physics of the device matching.
- **DC Goal Setter:** Acting as the biasing strategist, this agent translates the topology into quantitative DC operating targets. Instead of generic operating regions, it defines specific targets for Overdrive Voltage, Drain-Source Voltage, and Current Density for every transistor. It creates a global bias distribution plan, ensuring sufficient voltage headroom for signal swing and defining the necessary start-up conditions for the circuit to converge.
- **Initial Designer:** This agent generates the complete initial parameter set required to start the simulation. To guarantee executability, the workflow employs a dynamic Prompt Injection technique: it parses the raw netlist to extract all mandatory variables and forces the agent to populate exactly those keys, preventing parameter hallucination or omission. The agent prioritizes simulatability and convergence by selecting conservative, stable values aligned with the DC goals, ensuring the design serves as a valid starting point for subsequent numerical optimization phases.

We present the details of this phase in Fig. 1.B.

C. DC-OP Sizing

With previous analysis results, VLM-CAD initiates a preparatory second phase to establish a reasonable DC-biased solution before conducting costly performance simulations. During this phase, the goal is not to achieve perfect DC convergence, but to quickly gain insights into the circuit's behavior in the target technology using limited language model calls and simulations.

- **DC Reviewer:** This agent serves as the validation gate-keeper, orchestrating a fast DC operating point SPICE simulation focusing on the target output node DC level to ensure proper biasing. It extracts node voltages and device operating points and compares these against the DC goals from previous analysis, generating a structured discrepancy report that quantifies headroom violations and region errors. It calculates a discrepancy count that serves as the stopping criterion for the optimization loop.
- **DC Sizer:** This agent executes the inferencing-based parameter refinement. It ingests the discrepancy report and applies analog design heuristics to resolve biasing issues. Notably, we enforce full-set consistency here to ensure that static testbench parameters, matching constraints and physical range limits are strictly preserved across iterations, preventing simulation divergence.

We present the details of this phase in Fig. 1.C.

D. Inference-Only Sizing

After refining the DC-OP sizing, we proceed to optimize all the necessary specifications through full simulations. During this phase, VLM-CAD relies exclusively on the inherent knowledge of analog circuit theory provided by language models, along with context from previous agents, to enhance the design without any external numerical optimizers. With sample-efficient loops, this phase aims to swiftly find optimal designs before resorting to simulation-intensive optimizers.

To transform the multi-objective analog circuit sizing task into a scalar optimization task suitable for both the language model agents and the numerical optimizer, we define a **Universal Cost Function**, denoted as $J(\mathbf{x})$, to guide the search through two distinct phases: **Feasibility** and **Optimization**. The Feasibility phase aims to satisfy all specifications except for power, while the Optimization phase focuses on minimizing power consumption. For a given set of design parameters \mathbf{x} , we define the Universal Cost Function as follows:

$$J(\mathbf{x}) = \frac{P_{\text{meas}}(\mathbf{x})}{P_{\text{max}}} + \sum_{i \in \mathcal{S}} w_i \cdot \mathcal{V}_i(y_i, T_i) + \mathcal{P}_{\text{sanity}}. \quad (1)$$

Here:

- P_{meas} is the simulated power consumption and P_{max} is the maximum allowable power specification.
- \mathcal{S} represents the set of all performance metrics. We divide this set into lower-bound specifications \mathcal{S}_{LB} , such as gain and PM, and upper-bound specifications \mathcal{S}_{UB} , such as THD and offset.

- w_i represents the penalty weight for metric i , prioritizing critical specs.
- \mathcal{V}_i is the Rectified Linear Unit (ReLU) violation function. We define \mathcal{V}_i as follows to handle the directionality of different specifications rigorously:

$$\mathcal{V}_i(y_i, T_i) = \begin{cases} \max(0, T_i - y_i), & i \in \mathcal{S}_{LB} \\ \max(0, y_i - T_i), & i \in \mathcal{S}_{UB}. \end{cases} \quad (2)$$

- $\mathcal{P}_{\text{sanity}}$ is a significant constant penalty applied only when fundamental functionality is compromised, such as non-convergence or near-zero gain, serving as a soft barrier to guide the search away from non-functional areas.

This formulation creates a smooth optimization landscape: when $J(\mathbf{x}) > 1$, the agents focus on satisfying all specifications except for power (Feasibility Mode). Once $J(\mathbf{x}) \leq 1$, the logic naturally transitions to minimizing power while maintaining compliance (Optimization Mode).

We present the details of this phase in Fig. 1.D:

- **Specs Reviewer:** This agent functions as a rigorous validation engine, using a hybrid DC/AC simulation strategy combined with a Skip-on-Fail mechanism to evaluate design performance efficiently. Instead of performing computationally expensive simulations indiscriminately, it first verifies the DC operating point. If the circuit fails basic biasing checks, the process is halted early to conserve resources. Once the simulation is successful, it computes $J(\mathbf{x})$, which quantifies the design's compliance with the specifications and serves to assess the optimization status.
- **Language Model Inferencing Sizer:** This agent performs parameter refinement based on inferencing, utilizing a history-aware context window to avoid optimization oscillation. Guided by $J(\mathbf{x})$, it dynamically alternates between strategies for satisfying constraints and minimizing power consumption. To ensure robustness against stagnation, the workflow includes a dead loop detection and perturbation mechanism: if the agent suggests a parameter set identical to the previous iteration, the system automatically applies a 5% random perturbation to transistor widths, which disrupts the inferencing deadlock and propels the simulator into a new state, enabling the optimization process to regain momentum.

E. ExTuRBO Sizing and Explaining

When inference-only sizing reaches its iteration limit or convergence plateau, we escalate to the final optimization stage, where VLM-CAD transitions from qualitative inferencing to quantitative precision.

We propose **ExTuRBO**, an Explainable Trust Region Bayesian Optimization method to bridge the gap between language models and black-box optimization. Unlike standard TuRBO, we design ExTuRBO with two unique features:

- **Collaborative Warm-Starting:** Standard TuRBO initializes with a Latin Hypercube Sampling of the entire

high-dimensional search space, which wastes significant simulation budget exploring non-functional regions. ExTuRBO, conversely, is seeded by the agents. We extract the unique set of high-performing candidates \mathcal{D}_{seed} from the inference-only sizing phase.

The Trust Regions for the parallel independent workers are initialized centering on these seeds:

$$\mathbf{x}_{center}^{(0)} = \arg \min_{\mathbf{x} \in \mathcal{D}_{seed}} J(\mathbf{x}). \quad (3)$$

This initialization allows the numerical optimizer to perform local fine-tuning starting immediately from a feasible design point found by the language models.

- **Dual-Granularity Explainability:** To provide ground-truth explainability required for the final design report, ExTuRBO utilizes Automatic Relevance Determination (ARD). We define the kernel function as follows:

$$k(\mathbf{x}, \mathbf{x}') = \sigma_f^2 \exp \left(- \sum_{d=1}^D \frac{(x_d - x'_d)^2}{2\ell_d^2} \right). \quad (4)$$

Here, ℓ_d is the lengthscale of parameter d . We define the Feature Importance S_d as the inverse lengthscale: $S_d \propto 1/\ell_d$, as a small ℓ_d implies high sensitivity.

ExTuRBO fits two distinct GP models post-optimization to generate insights: **Global Sensitivity**, which we fit on the entire dataset and identifies survival parameters that determine basic circuit feasibility, and **Elite Sensitivity**, which we fit only on the top 15% of designs and identifies tuning parameters that drive high-performance metrics.

We present the details of this phase in Fig. 1.E:

- **Advisor Reviewer:** This agent acts as the bridge between the inference-only sizing phase and the numerical phase. It analyzes the optimization history and filters the iteration logs to identify the best unique candidates for seeding. It then configures ExTuRBO’s search bounds based on the stagnation context and explicitly triggers the external tool.
- **Equipped Sizer:** This agent serves as the execution interface for the numerical engine. It configures the parallel ExTuRBO workers with the seeds provided by the Advisor. Upon completion of the numerical run, it serves as the result explainer: it incorporates insights from Global Sensitivity and Elite Sensitivity, synthesizing them into a comprehensive design sign-off report that details the selected optimal parameters. Additionally, the report explains the rationale for these choices, distinguishing between parameters fixed for stability and those adjusted for enhanced performance.

IV. EXPERIMENTS

A. Experimental Setup

We utilize VLM-CAD to size two distinct circuits:

- 1) an amplifier with a complementary input and a class-AB output stage [26]. We size it using both the 180nm and 90nm BSIM predictive technology models [10].

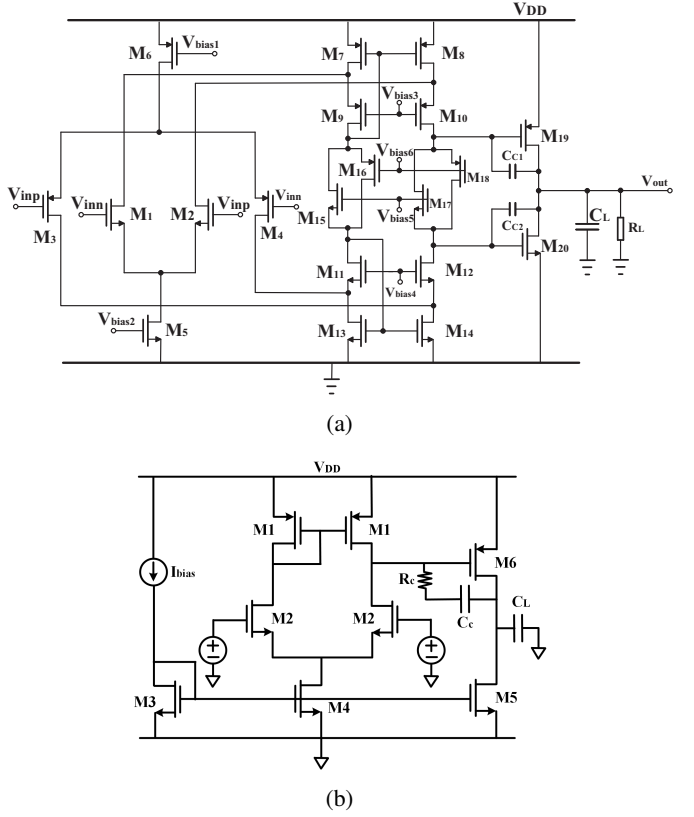


Fig. 3: Schematics of the two amplifiers we use in our experiments: (a) an amplifier with complementary input and a class-AB output stage, (b) a two-stage Miller operational amplifier.

- 2) a two-stage Miller operational amplifier [25]. We size it using the 45nm BSIM predictive technology model [10].

We demonstrate both circuits in Fig. 3. We use Gemini 3 Flash Preview as the VLM and Ngspice [9] for all simulations here. We conduct all our experiments on a server powered by an AMD® EPYC™ 9654 CPU with 32 cores allocated.

We consider six specification constraints for optimization: Gain, Phase Margin (PM), Unity Gain Bandwidth (UGBW), Total Harmonic Distortion (THD), Input Offset, and Power. We aim to minimize power consumption while satisfying all five other specification constraints. We define the ranges for the sizing parameters, summarized in TABLE I.

For the Universal Cost Function, we use the following metric penalty weight: $w_{gain} = 1.0$, $w_{ugbw} = 0.2$, $w_{pm} = 0.1$, $w_{thd} = 0.5$, $w_{offset} = 10.0$. We set $\mathcal{P}_{sanity} = 100.0$. For each circuit, we conduct five independent optimization experiments. In each experiment, we set the following limits:

- Phase C has a maximum of 10 iterations to find a reasonable DC-biased solution,
- Phase D is limited to 40 iterations until the universal cost reaches 0.5,
- ExTuRBO of Phase E has a maximum budget of 400 iterations to achieve a universal cost of 0.5, followed by an additional 40 iterations to reduce power consumption.

TABLE I: Sizing parameter ranges for the two amplifiers we use in our experiments.

(a) Ranges for the amplifier with a complementary input and a class-AB output stage. (b) Ranges for the two-stage Miller operational amplifier.

Parameter	180nm	90nm	Parameter	45nm
Width (μm)	[0.18, 400]	[0.09, 400]	Width (μm)	[0.25, 5]
Length (μm)	[0.18, 18]	[0.09, 9]	Length (nm)	[45, 225]
Bias Voltage (V)	(0, 1.8)	(0, 1.2)	Mult	[1, 25]
Supply Volt. (V)	1.8	1.2	Supply Volt. (V)	1.2
Comp. Cap. (pF)	[1, 10]	[1, 10]	Comp. Cap. (pF)	[0.1, 10]
Load Cap. (pF)	10	10	Load Cap. (pF)	10
Load Res. ($\text{k}\Omega$)	1	1	Bias Current (μA)	30

B. Results and Analysis

We present the optimization results of VLM-CAD in TABLE II and the average runtime in TABLE III. For optimization of the amplifier with a complementary input and a class-AB output stage, VLM-CAD achieves a total runtime of under 9 minutes. For optimization of the two-stage Miller operational amplifier, VLM-CAD achieves a total runtime of under 43 minutes. Both sets of experiments demonstrate that VLM-CAD significantly outperforms existing approaches regarding total runtime. VLM-CAD successfully optimizes the amplifier with a complementary input and a class-AB output stage. It achieves a 100% success rate, meets all specification requirements, and maintains low power consumption in every attempt.

Nevertheless, for the two-stage Miller operational amplifier, VLM-CAD fails to meet all specification requirements, particularly regarding Gain and PM, and it exceeds the allowable power consumption. This discrepancy arises from the significantly different sizes of the feasible design spaces for the two circuits. The amplifier with a complementary input and a class-AB output stage provides a relaxed power budget and less stringent linearity requirements, resulting in a wide solution space where many parameter combinations can achieve the desired outcomes. In contrast, the two-stage Miller operational amplifier presents a highly constrained optimization problem. The combination of stringent fidelity requirements and a tight double-sided power constraint effectively creates a tiny target area within the search space, making it difficult for VLM-CAD to pinpoint the precise solution, as the design margins in the 45nm simple topology are limited.

We also present a case of the final design report in Fig. 4. For the final design report, we include both Global Sensitivity and Elite Sensitivity analyses provided by ExTuRBO, along with explanations based on these analyses from the Equipped Sizer. By offering quantified sensitivity to the language model, we significantly reduce the risk of generating incorrect explanations.

C. Ablation Study

To demonstrate the significance of circuit schematics and the assistance of Image2Net in helping VLM interpret them, we conduct ablation studies in two distinct paradigms:

TABLE II: Optimization results for the two amplifiers we use in our experiments. The red fonts denote metrics that did not meet the specification requirements.

(a) Optimization results for the amplifier with a complementary input and a class-AB output stage.

PTM	Run	Gain (dB)	UGBW (MHz)	PM (°)	THD (dB)	Offset (mV)	Power (mW)
Target	-	≥ 65	≥ 10	≥ 50	≤ -26	≤ 1	≤ 10
180nm	1	88.657	17.736	54.497	-114.935	0.966	1.074
	2	84.866	30.075	51.399	-92.188	0.901	3.290
	3	86.200	13.388	56.349	-100.581	0.067	3.424
	4	85.505	35.111	51.897	-94.375	0.551	0.810
	5	73.827	12.300	56.862	-107.192	0.617	1.399
90nm	1	94.883	18.388	70.283	-93.027	0.526	2.321
	2	71.808	32.183	52.374	-95.270	0.997	0.366
	3	86.780	47.386	70.031	-107.083	0.947	0.599
	4	85.735	89.300	56.387	-98.704	0.837	0.599
	5	89.004	68.229	62.407	-113.503	0.985	0.379

(b) Optimization results for the two-stage Miller operational amplifier.

PTM	Run	Gain (dB)	UGBW (MHz)	PM (°)	THD (dB)	Offset (mV)	Power (μW)
Target	-	≥ 54	≥ 1	≥ 60	≤ -60	≤ 5	$45 \leq P \leq 85$
45nm	1	53.544	7.224	39.866	-70.408	1.659	128.189
	2	53.295	12.733	24.478	-85.431	3.236	92.800
	3	51.047	3.338	166.722	-69.335	3.470	76.308
	4	53.180	1.523	48.703	-77.933	3.838	68.321
	5	50.971	1.905	72.065	-83.100	3.387	307.312

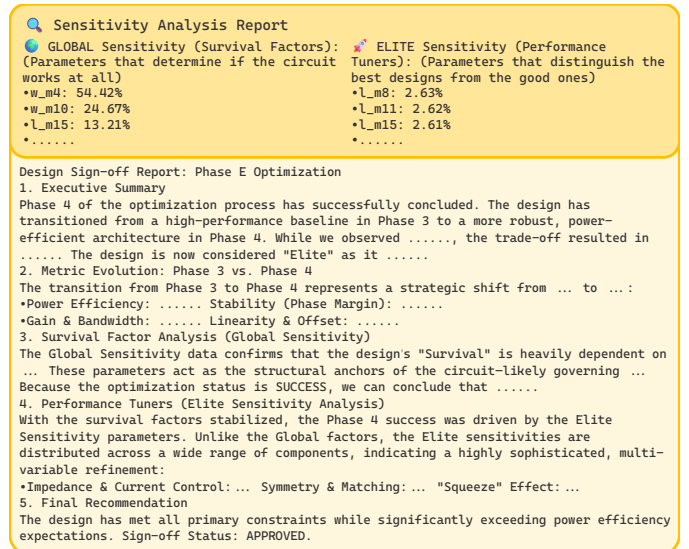


Fig. 4: Final design report that includes Global Sensitivity, Elite Sensitivity, and explanations based on these quantified data.

TABLE III: Average runtime for the optimization of the two amplifiers we use in our experiments. The **red** and **blue** fonts indicate the shortest and the second shortest average runtime, respectively.

(a) Average runtime for the optimization of the amplifier with a complementary input and a class-AB output stage.

PTM	Phase A		Phase B		Phase C		Phase D		Phase E		Total
	Time (s)	Time (s)	Time (s)	Iter	Time (s)	Iter	Time (s)	Seed	Time (s)		
180nm	VLM-CAD	13.58 \pm 1.38	119.26 \pm 19.93	1.0 \pm 0.0	6.62 \pm 0.67	13.4 \pm 14.1	91.28 \pm 106.22	2.0 \pm 0.9	159.06 \pm 71.23	389.80 \pm 122.28	
	Ablation 1	-	102.66 \pm 6.67	1.0 \pm 0.0	13.62 \pm 8.88	24.8 \pm 18.6	183.18 \pm 147.42	2.4 \pm 0.8	1137.94 \pm 897.04	1437.40 \pm 984.50	
	Ablation 2	-	75.48 \pm 7.14	1.0 \pm 0.0	9.38 \pm 3.93	13.8 \pm 13.7	88.96 \pm 108.14	2.4 \pm 0.8	646.52 \pm 623.37	820.34 \pm 608.73	
90nm	VLM-CAD	13.70 \pm 0.83	95.86 \pm 9.03	1.0 \pm 0.0	6.50 \pm 0.21	1.8 \pm 1.2	9.16 \pm 10.86	1.4 \pm 0.8	138.04 \pm 16.00	263.26 \pm 22.55	
	Ablation 1	-	96.60 \pm 16.39	1.0 \pm 0.0	6.12 \pm 0.70	2.0 \pm 1.3	178.12 \pm 8.39	1.8 \pm 1.0	2150.48 \pm 1151.21	2431.32 \pm 1150.02	
	Ablation 2	-	78.62 \pm 7.90	1.0 \pm 0.0	7.68 \pm 1.15	7.0 \pm 7.5	36.82 \pm 45.10	1.8 \pm 1.0	176.30 \pm 62.86	299.42 \pm 104.50	

(b) Average runtime for the optimization of the two-stage Miller operational amplifier.

PTM	Run	Phase A		Phase B		Phase C		Phase D		Phase E		Total
		Time (s)	Time (s)	Time (s)	Iter	Time (s)	Iter	Time (s)	Seed	Time (s)		
45nm	VLM-CAD	15.38 \pm 5.19	97.04 \pm 18.25	1.0 \pm 0.0	19.16 \pm 24.36	40.0 \pm 0.0	180.02 \pm 11.17	3.0 \pm 0.0	2120.92 \pm 88.18	2432.52 \pm 137.33		
	Ablation 1	-	96.60 \pm 16.39	1.0 \pm 0.0	6.12 \pm 0.70	40.0 \pm 0.0	178.12 \pm 8.39	3.0 \pm 0.0	2545.16 \pm 710.06	2826.00 \pm 702.45		
	Ablation 2	-	69.90 \pm 5.21	1.0 \pm 0.0	5.48 \pm 0.56	40.0 \pm 0.0	147.90 \pm 14.77	3.0 \pm 0.0	2277.00 \pm 154.01	2500.28 \pm 165.34		

TABLE IV: Ablation study 1 results for the two amplifiers with only the original schematic input. The **red** fonts denote metrics that did not meet the specification requirements.

(a) Ablation study 1 results for the amplifier with a complementary input and a class-AB output stage, with only the original circuit schematic input.

PTM	Run	Gain (dB)	UGBW (MHz)	PM (°)	THD (dB)	Offset (mV)	Power (mW)
Target	-	≥ 65	≥ 10	≥ 50	≤ -26	≤ 1	≤ 10
180nm	1	91.425	20.753	120.509	-130.044	0.502	0.743
	2	88.862	10.822	52.935	-103.214	0.813	0.231
	3	68.606	18.973	51.560	-121.845	0.725	1.908
	4	69.873	24.221	51.046	-104.489	0.847	1.767
	5	67.447	73.455	111.363	-80.279	0.138	3.120
90nm	1	74.210	62.115	67.292	-68.112	0.591	1.588
	2	75.264	117.800	147.976	-66.165	0.003	2.847
	3	88.201	83.296	60.460	-109.750	0.996	0.622
	4	88.425	50.652	70.540	-112.130	0.918	0.269
	5	96.313	51.232	63.462	-111.572	0.870	0.250

(b) Ablation study 1 results for the two-stage Miller operational amplifier with only the original circuit schematic input.

PTM	Run	Gain (dB)	UGBW (MHz)	PM (°)	THD (dB)	Offset (mV)	Power (μ W)
Target	-	≥ 54	≥ 1	≥ 60	≤ -60	≤ 5	$45 \leq P \leq 85$
45nm	1	45.491	5.960	179.214	-76.714	3.529	111.095
	2	54.729	1.615	42.124	-90.886	2.117	64.008
	3	54.253	7.166	25.349	-79.876	2.823	69.961
	4	54.806	0.808	72.862	-79.515	0.549	71.493
	5	53.937	1.203	43.184	-73.218	4.769	51.445

- 1) Input only original circuit schematic, with no annotated schematic and JSON description.
- 2) Input no circuit schematic information at all.

We present our ablation study results and runtime in TABLE III-V and Fig. 5. Our observations indicate that both ablation paradigms for the amplifier with a complementary input and a class-AB output stage meet all specification requirements most of the time, demonstrating the robustness of VLM-CAD. However, ablation studies on both circuits require significantly longer runtimes than VLM-CAD, primarily due

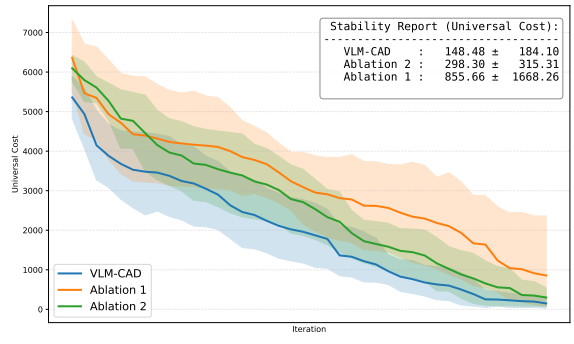


Fig. 5: Universal cost distribution of Phase 3 for the two-stage Miller operational amplifier, organized from highest to lowest costs.

to Phase E. We believe this is due to the additional information on components and their connections, which supports a better analysis in Phase B and, consequently, provides better seeds for Phase E to optimize.

Additionally, we notice that ablation study 1 runs longer on average than ablation study 2. Furthermore, we reorganize the universal costs for each iteration in Phase 3 of the two-stage Miller operational amplifier, ranking them from high to low. We visualize the results (see Fig. 5) and calculate their average and standard deviation. We observe that the universal cost of ablation study 1 is significantly higher and more unstable than that of ablation study 2 and VLM-CAD. Both discrepancies arise because we conduct ablation 1 using only the original schematic input. Given that VLM struggles to interpret circuit schematics, this input effectively acts as an adversarial image. Consequently, under visual adversarial attacks, the VLM generates worse seeds than in ablation study 2 [8], leading to longer optimization times during Phase E.

V. CONCLUSION

We propose VLM-CAD, a VLM-optimized collaborative agent design workflow. By leveraging Image2Net to aid VLM

TABLE V: Ablation study 2 results for the two amplifiers with only the original schematic input. The **red** fonts denote metrics that did not meet the specification requirements.

(a) Ablation study 2 results for the amplifier with a complementary input and a class-AB output stage, with only the original circuit schematic input.

PTM	Run	Gain (dB)	UGBW (MHz)	PM (°)	THD (dB)	Offset (mV)	Power (mW)
Target	-	≥ 65	≥ 10	≥ 50	≤ -26	≤ 1	≤ 10
180nm	1	87.207	44.295	8.851	-92.001	0.574	2.799
	2	85.420	45.644	55.955	-80.911	0.928	5.866
	3	92.871	14.304	50.480	-123.744	0.272	1.143
	4	90.765	13.447	52.568	-139.373	0.018	3.176
	5	93.884	18.547	54.123	-97.836	0.914	0.307
90nm	1	89.596	82.470	63.058	-108.417	0.728	0.656
	2	89.963	165.218	49.885	-100.876	0.680	1.133
	3	88.727	95.892	53.486	-110.764	0.767	0.496
	4	90.169	60.224	50.136	-104.568	0.653	2.893
	5	94.623	73.014	62.141	-92.835	0.789	1.785

(b) Ablation study 2 results for the two-stage Miller operational amplifier with only the original circuit schematic input.

PTM	Run	Gain (dB)	UGBW (MHz)	PM (°)	THD (dB)	Offset (mV)	Power (μ W)
Target	-	≥ 54	≥ 1	≥ 60	≤ -60	≤ 5	$45 \leq P \leq 85$
45nm	1	53.948	13.076	16.848	-80.262	3.902	93.733
	2	54.625	10.714	24.372	-81.814	3.720	83.984
	3	50.481	10.700	12.239	-74.654	2.433	80.723
	4	52.783	10.538	17.477	-76.923	2.524	115.607
	5	53.274	9.688	28.079	-92.373	4.440	97.477

in interpreting circuit schematics and ExTuRBO for explainable, warm-started optimization, VLM-CAD effectively reduces the risks of hallucination and the lack of transparency that are often seen in existing approaches. Experiment results across multiple PTMs demonstrate VLM-CAD’s robustness in satisfying stringent specifications while minimizing power, achieving a 100% success rate in optimizing an amplifier with a complementary input and a class-AB output stage while maintaining total runtime under 43 minutes across all experiments. The final design reports, including a quantified sensitivity analysis, effectively bridge the gap between automated optimization and designer trust, marking a step toward reliable agentic automatic analog circuit sizing.

REFERENCES

- [1] P. Rahmanzadehgervi, L. Bolton, M. R. Taesiri, and A. T. Nguyen, “Vision language models are blind,” in Proc. Asian Conf. Computer Vision (ACCV), Dec. 2024, pp. 18–34.
- [2] D. V. Kochar, H. Wang, A. P. Chandrakasan, and X. Zhang, “LEDRO: LLM-Enhanced Design Space Reduction and Optimization for Analog Circuits,” in Proc. IEEE Int. Conf. LLM-Aided Design (ICLAD), 2025, pp. 141–148.
- [3] S. Xu, H. Zhi, J. Li, and W. Shan, “LLMACD: An LLM-Based Analog Circuit Designer Driven by Behavior Parameters,” in 2025 International Symposium of Electronics Design Automation (ISEDA), 2025, pp. 157–162.
- [4] C. Liu, W. Chen, A. Peng, Y. Du, L. Du, and J. Yang, “AmpAgent: An LLM-based Multi-Agent System for Multi-stage Amplifier Schematic Design from Literature for Process and Performance Porting,” arXiv:2409.14739, 2024.
- [5] M. Ahmadzadeh, K. Chen, and G. Gielen, “(Invited Paper) AnaFlow: Agentic LLM-based Workflow for Reasoning-Driven Explainable and Sample-Efficient Analog Circuit Sizing,” in ICCAD, 2025, pp. 1–7.
- [6] Z. Zhao, A. Daiv, and D. Porras, “CURVLM: Circuit Understanding Via Group Relative Policy Optimization (GRPO) on Vision Language Models,” CS231n: Deep Learning for Computer Vision, Stanford, Final Project Reports, Highlight, Spring 2025.
- [7] Anonymous, “SchemixQA and CoRe-VLM: A Benchmark and Collaborative Refinement (CoRe) Framework for Visual Question Answering on Technical Schematics,” in Submitted to The Fourteenth International Conference on Learning Representations, 2025, under review.
- [8] X. Cui, A. Aparcero, Y. K. Jang, and S.-N. Lim, “On the Robustness of Large Multimodal Models Against Image Adversarial Attacks,” in Proc. IEEE/CVF Conf. Comput. Vis. Pattern Recognit. (CVPR), June 2024, pp. 24625–24634.
- [9] H. Vogt, G. Atkinson, P. Nenzi, and D. Warning, Ngspice User’s Manual Version 43 (Ngspice Release Version), 2024.
- [10] Y. Cao, Predictive Technology Model for Robust Nanoelectronic Design, 1st ed. New York, NY: Springer, 2011, pp. XV–173.
- [11] A. Girardi, T. De-Oliveira, S. Ghismoni, P. C. Aguirre, and L. Compassi-Severo, “A comprehensive review on automation-based sizing techniques for analog IC design,” J. Integr. Circuits Syst., vol. 17, no. 3, pp. 1–14, 2022.
- [12] M. Taherzadeh-Sani, R. Lotfi, H. Zare-Hoseini, and O. Shoaei, “Design optimization of analog integrated circuits using simulation-based genetic algorithm,” in Signals, Circuits and Systems, 2003. SCS 2003. International Symposium on, vol. 1, 2003, pp. 73–76.
- [13] K. Touloupas and P. P. Sotiriadis, “LoCoMOBO: A Local Constrained Multiobjective Bayesian Optimization for Analog Circuit Sizing,” IEEE Trans. Comput.-Aided Design Integr. Circuits Syst., vol. 41, no. 9, pp. 2780–2793, 2022.
- [14] K. Settaluri, A. Haj-Ali, Q. Huang, K. Hakhamaneshi, and B. Nikolic, “AutoCkt: Deep Reinforcement Learning of Analog Circuit Designs,” in 2020 Design, Automation & Test in Europe Conference & Exhibition (DATE), 2020, pp. 490–495.
- [15] H.-Y. Hsu and M. P.-H. Lin, “Automatic Analog Schematic Diagram Generation based on Building Block Classification and Reinforcement Learning,” in Proceedings of the 2022 ACM/IEEE Workshop on Machine Learning for CAD, Virtual Event, China, 2022, pp. 43–48.
- [16] Y. Bang, Z. Ji, A. Schelten, A. Hartshorn, T. Fowler, C. Zhang, N. Cancedda, and P. Fung, “HalluLens: LLM Hallucination Benchmark,” arXiv:2504.17550, 2025.
- [17] M. T. M. Emmerich, K. C. Giannakoglou, and B. Naujoks, “Single- and multiobjective evolutionary optimization assisted by Gaussian random field metamodels,” IEEE Trans. Evol. Comput., vol. 10, no. 4, pp. 421–439, 2006.
- [18] Z. Wu, Z. Chen, N. Achebe, V. V. Rao, P. Shrestha, and I. Savvidis, “Emerging ML-AI Techniques for Analog and RF EDA,” arXiv:2506.00007, 2025, pp. 9.
- [19] K. G. Liakos and F. Plessas, “Analog Design and Machine Learning: A Review,” Electronics, vol. 14, no. 17, p. 3541, 2025.
- [20] L. Skelic, Y. Xu, M. Cox, W. Lu, T. Yu, and R. Han, “CIRCUIT: A Benchmark for Circuit Interpretation and Reasoning Capabilities of LLMs,” arXiv:2502.07980, 2025.
- [21] I. Terpstra, “Empowering Analog Integrated Circuit Design through Large Language Models and Reinforcement Learning,” M.Eng. thesis, Dept. Elect. Eng. Comput. Sci., Massachusetts Institute of Technology, Cambridge, MA, USA, 2024.
- [22] B. Razavi, “Analog Design Experiments With AI—Part 1 [The Analog Mind],” IEEE Solid-State Circuits Mag., vol. 17, no. 4, pp. 11–15, 2025.
- [23] M. Ahmadzadeh, J. Lappas, N. Wehn, and G. Gielen, “AnaCraft: Duel-Play Probabilistic-Model-based Reinforcement Learning for Sample-Efficient PVT-Robust Analog Circuit Sizing Optimization,” IEEE Trans. Comput.-Aided Des. Integr. Circuits Syst., early access, 2025.
- [24] C. Liu and D. Chitnis, “EEsizer: LLM-Based AI Agent for Sizing of Analog and Mixed Signal Circuit,” IEEE Trans. Circuits Syst. I, Reg. Papers, pp. 1–10, 2025.
- [25] M. Ahmadzadeh, J. Lappas, N. Wehn, and G. Gielen, “AnaCraft: Duel-Play Probabilistic-Model-based Reinforcement Learning for Sample-Efficient PVT-Robust Analog Circuit Sizing Optimization,” IEEE Trans. Comput.-Aided Des. Integr. Circuits Syst., early access, 2025.
- [26] C. Liu and D. Chitnis, “EEsizer: LLM-Based AI Agent for Sizing of Analog and Mixed Signal Circuit,” IEEE Trans. Circuits Syst. I, Reg. Papers, pp. 1–10, 2025.